City and Environment Interactions 32 (2026) 100507

Contents lists available at ScienceDirect

City and Environment Interactions

journal homepage: www.sciencedirect.com/journal/city-and-environment-interactions

Effect of shade and surface material on thermal conditions in California schoolyards

Luisa Velasquez-Camacho [a,*], Natalie S. van Doorn [b], Lara A. Roman [c], Iryna Dronova [d], Kirsten Schwarz [e,f], Jared Sisneroz [a], Elizabeth Riedman [f], Levon M. Bigelow [g], Alessandro Ossola [a]

[a] Department of Plant Sciences, University of California Davis, Davis, CA, USA
[b] USDA Forest Service, Pacific Southwest Research Station, Albany, CA, USA
[c] USDA Forest Service, Pacific Southwest Research Station, San Diego, CA, USA
[d] Departments of Environmental Science, Policy and Management, and Landscape Architecture & Environmental Planning, University of California, Berkeley, CA, USA
[e] Department of Environmental Health Sciences, University of California, Los Angeles, CA, USA
[f] Department of Urban Planning, University of California, Los Angeles, CA, USA
[g] Oak Ridge Institute for Science and Education with the USDA Forest Service, Pacific Southwest Research Station, Sacramento, CA, USA

ARTICLE INFO

Keywords:
Temperature
Heat index
Urban microclimate
Asphalt
Artificial turf
Tree shade
School landscape

ABSTRACT

Schoolyards represent a critical asset for mitigating climate-related heat exposure among children. Young children in elementary school are a group particularly vulnerable to rising temperatures, heat waves, and prolonged exposure to high thermal stress. Such pupils are more susceptible to heat due to their physiological characteristics and the amount of time they spend outdoors during school hours. Consequently, schoolyard design, including the surface materials used and the provision of both natural and artificial shade, plays a key role in ensuring children's thermal safety. Despite this importance, relatively few studies have examined how combinations of surface materials and shade types influence heat in school environments. In this study, we evaluated summer microclimatic conditions in 8 elementary schools distributed across California, collecting continuous measurements during typical hours when children are present for school as well as after school programming (08: 30–17: 00). Air temperature and heat index were measured at approximately 0.7 m above ground using Kestrel sensors, representing the median height of an elementary student's chest. We applied generalized additive models (GAMs) to test how surface materials, shade, and shade type (natural/artificial) affect thermal conditions within schoolyards. While accounting for geographic and climatic variability, our analysis highlights consistent thermal patterns. Across schools, four sites frequently experienced heat index values within the 27–32 °C "caution" category during school hours, particularly in inland regions. Surface materials showed consistent differences in thermal exposure: metal structures and artificial turf exhibited the highest heat index values, exceeding cooler surfaces such as grass, PVC mats, and asphalt by more than 2 °C. However, each of these materials was measured by a single sensor at a single school, so these differences should not be interpreted as generalizable rankings. Shade was consistently associated with lower recorded near-surface air temperature and heat index relative to sun-exposed locations, with a median difference of ~1.2 °C in air temperature and ~ 1.4 °C in heat index (range: 0.2–2.4 °C and 0.3–2.4 °C, respectively). These findings support the need for climate-responsive schoolyard planning that considers the interactions between shade type and surface materials when trying to reduce children's heat exposure.

1. Introduction

Children spend over 30% of their daytime hours at school, and much of that time is spent outside [1]. Recess alone accounts for approximately 10–20% of children's daily moderate-to-vigorous physical activity and can represent up to 30–40% of total school-day physical activity [2,3]. Consequently, schoolyards function not only as educational spaces but also as key environments that directly influence

* Corresponding author.
E-mail address: lfvelasquez@ucdavis.edu (L. Velasquez-Camacho).

https://doi.org/10.1016/j.cacint.2026.100507
Received 4 June 2026; Received in revised form 20 October 2026; Accepted 20 October 2026
Available online 23 October 2026
2590-2520/© 2026 The Author(s). Published by Elsevier Ltd. This is an open access article under the CC BY license (http://creativecommons.org/licenses/by/4.0/).

children's health, safety, and overall well-being [4].

Playground and schoolyard configurations vary widely across cities and school districts, reflecting differences in regional climate, design standards, maintenance practices, socioeconomic context, and historical development [4,5]. As a result, schoolyards typically comprise a heterogeneous mix of surface materials [6]. Asphalt and concrete are generally the most prevalent surfaces, followed by grass, mulch, and artificial materials such as rubber or plastic tiles [7]. In smaller proportions, bare soil and metal structures are also commonly present [8]. The materials used in schoolyard design substantially modify thermal exposure, with heat stress varying by season and time of day [4].

The thermal properties of surface materials have been widely studied, particularly a given material's capacity to absorb heat during the daytime and release heat during the nighttime [9]. These characteristics play a critical role in shaping local microclimatic conditions [10]. However, despite the extensive body of research on surface materials, relatively few studies have focused specifically on school campuses [1]. In a study of schoolyard heat islands in Canada, Moogk-Soulis [11] found that schoolyard surface temperatures were consistently hotter than surrounding streets. Specifically, schoolyard surfaces can reach more than 30 °C higher than the air temperature when they are exposed to full sun [11]. However, most microclimate studies evaluating surface materials have been conducted in urban streets, parks, or other public spaces [12,13], rather than in school environments, where children spend long periods outdoors during peak daytime heat. Existing studies in school settings have typically researched overall heat perception [1] or the benefits of greening interventions [14].

There is a need to compare multiple surface materials across and between campuses systematically to more effectively integrate microclimate considerations into the design of children's outdoor spaces, including playgrounds and schoolyards [15,16]. Previous works have shown that schoolyards dominated by impervious materials can reach higher surface and air temperatures than surrounding vegetated areas [11,17]. Yet, evidence comparing the relative thermal behaviour of common schoolyard surfaces remains limited. Schoolyards often combine heat-retaining materials with limited vegetation and shade, potentially exposing students to elevated thermal stress during warm seasons. This gap is particularly relevant given growing concerns about climate change, rising temperatures, and children's vulnerability to heat-related health risks [18].

Previous research has consistently highlighted the critical role of shade in moderating outdoor thermal environments and improving thermal comfort, with distinct roles of natural shade (tree canopies) and artificial shade (i.e., formed by human-designed structures). Beyond its biophysical function, shade has increasingly been recognized as a critical and unevenly distributed urban resource [19]. As cities continue to warm, access to effective shade is becoming both a priority for governments and a matter of environmental equity [20], particularly in essential public spaces such as schools, parks, and healthcare facilities. Empirical evidence from a range of contexts supports the cooling benefits of shaded environments, drawing on several bioclimatic indices to quantify thermal stress, including the Thom's Discomfort Index (combining dry and wet-bulb temperature to estimate perceived thermal discomfort), physiological equivalent temperature (PET; an index expressing perceived thermal stress as an equivalent air temperature under standardized reference conditions), and the Universal Thermal Climate Index (UTCI; which integrates air temperature, humidity, wind speed, and radiation to represent whole-body thermal stress). For instance, Georgi & Zafiriadis, [21], in a study of urban parks in Thessaloniki, Greece, reported reductions of up to 24% in air temperature and 16% in the discontent index under tree shade. Similarly, Gkaidatzi et al. [22] found that naturally shaded areas within schoolyards in Athens experienced reductions in air temperature between 08:00 and 16:00 during summer conditions.

However, the magnitude of cooling varies depending on the type and configuration of shading elements. In some cases, artificial shade provided by built structures can produce cooling effects comparable to, or even exceeding, those of tree shade, particularly under specific urban geometries and peak radiation conditions [23]. At the same time, other studies have reported relatively small or non-significant differences in PET between natural and artificial shade, suggesting similar performance in terms of perceived thermal stress under certain conditions [24]. Notably, the same study found that tree shade achieved greater reductions in air temperature and UTCI than a concrete shelter, underscoring that the effectiveness of shade can depend on the thermal metric considered. While indices such as PET or UTCI provide a more physiologically comprehensive assessment of thermal stress, their calculation requires additional inputs, for instance, mean radiant temperature (MRT) and wind speed, as well as assumptions about clothing insulation and metabolic rate, that typically demand specialized instrumentation beyond what is feasible for routine monitoring in school settings [25]. The heat index, by contrast, can be calculated directly from standard air temperature and relative humidity measurements, making it a more realistic metric for school-based monitoring. Beyond biophysical performance, distinguishing between natural and artificial shade is also relevant from a planning perspective, as these strategies differ in terms of implementation time, maintenance requirements, community preferences and policy feasibility in areas where shade is limited [23,26,27].

Beyond shade type, the cooling performance of vegetation varies substantially across species, age, and urban context due to differences in canopy structure and physiological processes [4]. As these authors further note, the cooling effectiveness of trees depends not only on their intrinsic characteristics but also on surrounding surface materials, building geometry, and urban density. Underlying this variability is a shared mechanism, shade does not cool the air directly. Rather, by reducing the solar energy absorbed by surfaces, it lowers surface temperatures and, in turn, the sensible heat flux transferred to the adjacent air [23,28]. Natural and artificial shade differ, however, in how they reduce this radiative load. Tree canopies are often porous, transmitting part of the incoming shortwave radiation while adding evapotranspirative cooling; engineered structures, by contrast, typically block radiation more completely but provide no evapotranspiration and, depending on their material properties, may re-emit absorbed heat as longwave radiation [4,23]. Further, complementary benefits of natural and artificial shade become especially critical in hot, dry summer conditions when precipitation and irrigation can become limited both for evaporative cooling and for support of living plants providing shade [28].

California provides a particularly relevant context for evaluating schoolyard heat exposure. By 2025, the population of children aged 0–9 years exceeded 5.8 million, representing roughly 11% of the state's population (Velasquez-Camacho et al. [12]; California Department of Public Health, 2024). Many public Californian schools are designed as one-story, open-air campuses with extensive outdoor circulation and activity spaces [29]. This campus typology emerged from historical and policy drivers together with California's historically mild climate, which made outdoor-oriented school layouts a practical design approach for much of the twentieth century [5]. However, over the past decade, increasingly frequent and severe heat events have revealed a growing mismatch between these outdoor-oriented campus designs and current thermal risk, making schoolyards a priority setting for climate-adaptation and heat-mitigation strategies [5,30].

Building on this evidence, we address three complementary research questions: 1) which surface types are associated with the highest near-surface thermal exposure across schoolyards, and how consistent is the relative importance of different surface materials when analyzed at the individual school level? 2) What is the magnitude of the shade-associated reduction of near-surface air temperature and heat index? And how is this reduction affected by natural and artificial shade type, different surface materials, and climate zone? 3) Is natural shade associated with lower air temperature and heat index than artificial shade? Based on previous studies, we expect impervious materials such as asphalt and concrete to be associated with higher thermal exposure

compared with vegetated surfaces. Additionally, shaded conditions are expected to consistently reduce thermal exposure relative to full sun. However, given the mixed evidence in the literature regarding differences between natural and artificial shade, we further examine whether tree shade provides additional cooling compared to built shading structures in schoolyard environments. By addressing these questions, we seek to quantify how surface materials and shade conditions interact to influence thermal exposure and heat stress in California schoolyards. More broadly, the results provide evidence that can support school planning, landscape design and climate adaptation strategies aimed at reducing children's heat exposure and improving thermal safety of outdoor learning and play environment.

2. Methods

2.1. Study area

We analyzed microclimatic conditions across eight public elementary schools distributed throughout California, United States (Table 1). The study sites included two schools in the San Bernardino Valley, two in the Greater Los Angeles metropolitan area, two in the San Francisco Bay Area, and two in the Greater Sacramento area (Fig. 1). School-specific locations and identities are withheld in accordance with school district policies.

All study regions experience Mediterranean-type climates characterized by hot, dry summers and mild, wetter winters, although strong coastal–inland gradients produce substantial regional variability across California. Summer temperatures are strongly influenced by marine air and coastal fog, which reduces incoming solar radiation and moderates temperatures near the coast, while inland valleys experience substantially higher summer heating due to greater solar exposure and reduced marine influence [31]. These gradients are reflected across the four study regions. The San Francisco Bay Area exhibits the strongest coastal moderation, with frequent summer fog and mild temperatures [32]. The Greater Los Angeles region also experiences coastal influence, although inland portions of the metropolitan area can reach substantially higher summer temperatures. In contrast, the San Bernardino Valley sits near the transition between hot-summer Mediterranean (Csa) and semi-arid steppe (Bsk) climates, sharing the intense summer heating of other inland regions but with reduced humidity and summer precipitation. This warm inland basin experiences some of the most intense summer heat in the study, and climate change projections indicate increasing frequency and severity of heat waves and extreme temperature events in the region [33]. The Greater Sacramento region, located within California's Central Valley, experiences some of the highest summer temperatures in the state due to its inland position and continental climate influence, resulting in prolonged dry summers with high solar radiation and limited evaporative cooling [34].

Every school was monitored over two consecutive days during July or August. These periods were selected to capture peak summer thermal conditions typical of school hours (Table 1). Notably, California public school classes begin in mid-August, and although the school day ends by 16:00 h in the districts we studied, many children remain on campus using the outdoor space during after-school programs. School campuses are actively used through summer camps, childcare programs, sports practices, and other after-school or community activities [35]. Consequently, children and staff continue to experience outdoor heat exposure on school grounds during the summer months and late afternoon hours (Afterschool [36,37]). By measuring during mid-to late summer, we aimed to capture present-day peak heat conditions and use them as analogs for the warmer temperatures projected to occur during late spring and early summer school months in the coming decades [38,39].

2.2. Field measurements

At each school, we deployed between 16 and 23 Kestrel Heat Stress tracking sensors (Model 5400 Heat Stress Tracker Pro), depending on school size, arrangement, and spatial complexity of the various school zones and land covers (Fig. 2). Sensor height was adjusted to represent elementary students' exposure following ISO 7243 guidance [40], which recommends measurements at the level of the abdomen/chest of the exposed individual. Accordingly, kestrel sensors were measured at ~0.7 m, which represents a typical height of an elementary student's chest. For purposes of this study, the schoolyard is defined as the area within the school fence, meaning that parking lots, street trees, and entryways outside of fences were excluded. However, trees bordering the schoolyard are still represented in the layout because such trees sometimes hang over and shade the schoolyard.

Sensor placement was designed to capture all possible combinations of surface type and shade conditions present within each schoolyard. Surface categories included common schoolyard materials such as asphalt, concrete, grass, artificial turf, rubber tiles, mulch, bare soil, plastic (often polypropylene or PVC surfaces installed over asphalt, typically found on basketball courts), and metal (commonly present in

Table 1
Descriptive characteristics of the schools studied. Weather data was retrieved from Weatherbit API (Weatherbit.io, [12]). Mean temp: mean temperature. Max temp: maximum temperature. Min temp: minimum temperature. RH: relative humidity. Mean temp 30 years: long-term climatological maximum temperature, defined as the average of historical maximum temperatures over 30 years. The number of surface types represents the number of individual surface types in each school (All school layouts are in the supplementary material). Canopy cover was derived from a field-based tree inventory conducted at each site, in which crown dimensions (north–south and east–west diameters) were measured for every tree present.

School number	Location	School area (m^2)	Distance to coast (km)	Number of surfaces types	Mean temp (°C)	Max temp (°C)	Min temp (°C)	Mean temp 30 years (°C)	RH (%)	Tree canopy cover (%)	Sampling Date in 2025 summer
1	San Bernardino Valley	40,500.8	60–80	4	24.7	29.0	19.2	36.1	45.8	10.4	July 21–22
2	San Bernardino Valley	37,857.2	60–80	6	26.9	31.9	18.9	35.5	40.1	2.8	July 23–24
3	Greater Los Angeles	29,902.1	0–20	6	21.7	24.4	17.8	27.9	65.2	6.9	July 28–29
4	Greater Los Angeles	35,771.4	0–20	6	24.4	27.9	18.7	28	63.3	23.3	July 30–31
5	San Francisco Bay Area	25,971.9	0–20	6	18.7	21.1	15.3	24.4	62.7	1.5	Aug 04–05
6	San Francisco Bay Area	33,123.6	0–20	7	21.4	25.6	16.7	24.4	64.4	12.2	Aug 06–07
7	Greater Sacramento	40,248.4	40–60	6	30.6	39.2	19.5	32.7	37.2	7.3	Aug 09–10
8	Greater Sacramento	40,114	40–60	5	25.6	34.1	16.0	30.5	49.2	15.7	Aug 11–12

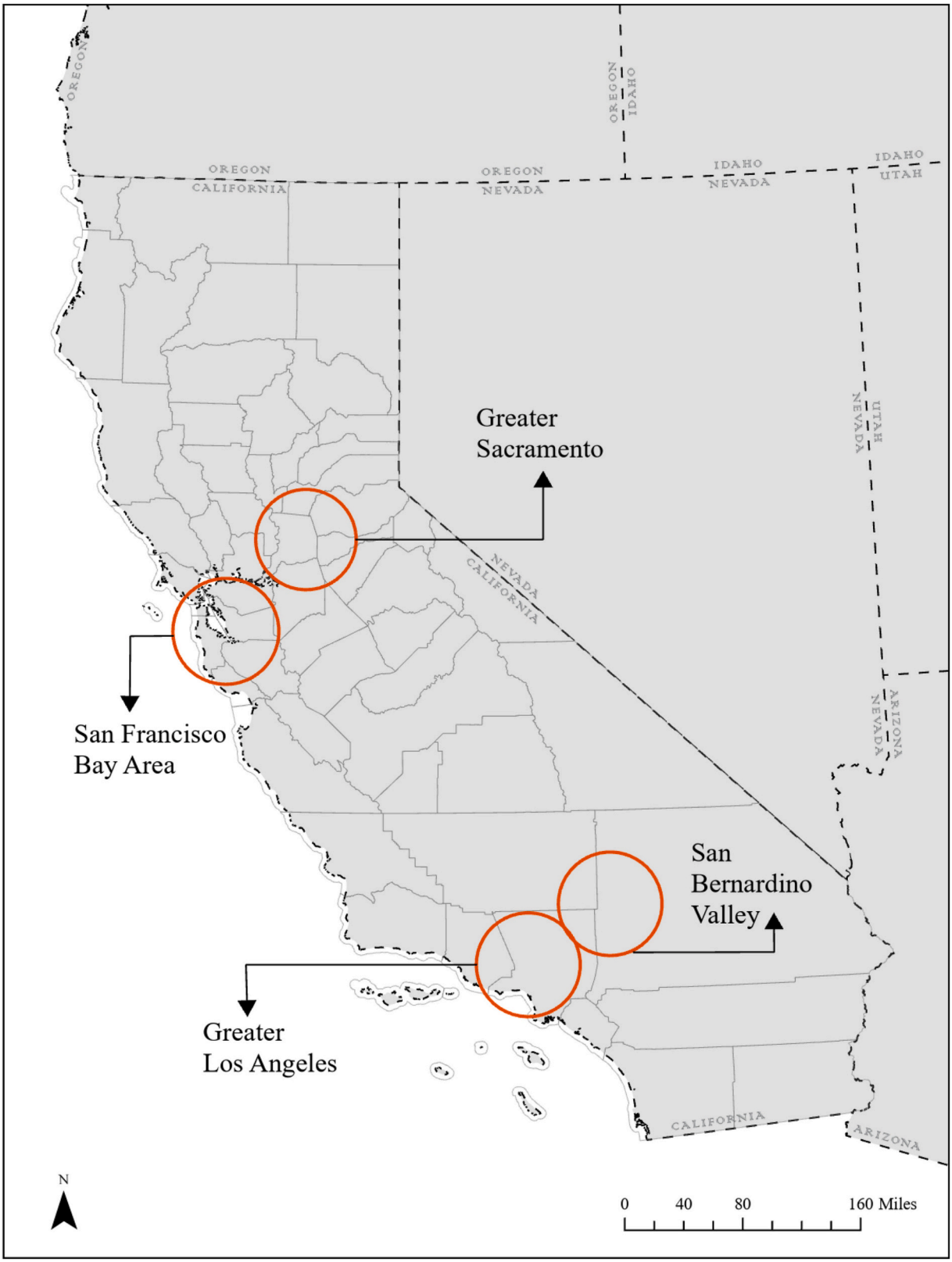


Fig. 1. General location of the study areas.

access platforms or ramps). Shade conditions were classified as shade, partial shade, and total sun exposure (Table 2). Partial shade designations were assigned based on direct field observation of each sensor location throughout the sampling day. The location was classified as partial shade when the shading element (tree canopy or built structure) covered the sensor during only part of the observation period, reflecting the diurnal movement of shade associated with changing solar angle. This classification therefore implicitly captures variation in the timing and extent of shade at the sensor level (e.g., morning-only or afternoon-only shading), although shade density or transmissivity was not



Fig. 2. Example of schoolyard layout and Kestrel sensor deployment in School 5. Complete layouts and sensor positions for all schools are provided in the Supplementary Material.

Table 2
Description of sensor location on different surface types and solar exposure conditions in School 5. Sensor positions for all schools are provided in the Supplementary Material.

Sensor number	Surface	Sun/Shade
K01	Asphalt	Sun
K02	Asphalt	Sun
K03	Asphalt	Partial shade - Artificial
K04	Asphalt	Sun
K05	Soil	Sun
K06	Soil	Sun
K07	Asphalt	Sun
K08	Rubber Tiles	Sun
K09	Rubber Tiles	Sun
K10	Rubber Tiles	Sun
K11	Rubber Tiles	Sun
K12	Rubber Tiles	Sun
K13	Rubber Tiles	Sun
K14	Rubber Tiles	Sun
K15	Rubber Tiles	Sun
K16	Grass	Shade - Artificial
K17	Asphalt	Sun
K18	Artificial turf	Shade - Natural
K19	Mulch	Partial shade – Natural
K20	Rubber Tiles	Sun
K21	Asphalt	Sun

quantified as a continuous variable. Shade was further differentiated by source as either natural (i.e., tree canopy) or artificial (e.g., buildings, shade structures, or other built elements). The assigned surface category corresponded to the dominant ground cover immediately surrounding each sensor.

It is important to note that schools are inherently diverse built environments, with surfaces, structures, and shade features constructed and rebuilt at different time periods using varying technologies and materials. Given this heterogeneity, our sampling approach was designed to capture this natural variability based on the specific characteristics present at each site, rather than impose a fully systematic and randomly replicated design that would be neither practical nor representative of real-world schoolyard conditions. While our study does not provide statistical replication across standardized conditions, we contend that even these single measurements at diverse sites can serve as an important baseline and minimal benchmark for future studies and thermal exposure assessments in school environments.

Measurements were collected every two minutes between 08:30 and 17:00 local time, corresponding to typical hours for school and after-school programs, and periods of highest thermal exposure for students and staff. Most measurements were conducted on mostly sunny days, albeit coastal areas (San Francisco Bay Area and Greater Los Angeles area) were affected by early morning fog that generally dissipated between 10:00 and 11:00. All study sites were located on relatively flat terrain, avoiding steep slopes or mountainous settings that could influence local microclimatic conditions. In addition, paired schools within each study region were located within relatively short distances of one another to ensure broadly comparable climatic conditions. Distances between paired schools were approximately 7 km in the Greater Sacramento region, 9 km in the San Bernardino Valley, 6.5 km in the Greater Los Angeles area, and 2.4 km in the San Francisco Bay Area.

2.3. Variables

We use the term thermal exposure to refer to the objective heat conditions captured by air temperature and the heat index, as distinct from thermal comfort, which additionally depends on factors such as wind speed, radiant heat, clothing, and metabolic activity and was not directly assessed in this study. To quantify thermal exposure, we used the heat index, which combines air temperature and relative humidity into a single measure of how hot the air feels, accounting for the reduced efficiency of evaporative cooling at higher humidity[41]. Widely used to assess health-relevant heat exposure in outdoor environments and to communicate heat risk to the public, the heat index provides an operationally meaningful complement to air temperature (National Weather Service, 2024). We therefore report both metrics throughout: near-surface air temperature for comparability with prior microclimate literature, and the heat index as the variable most relevant to public-health policy and risk communication.

Following U.S. National Weather Service classifications, heat index values were categorized into four risk levels: Caution (27–32 °C), Extreme Caution (32–41 °C), Danger (41–54 °C), and Extreme Danger (>54 °C). Increasing heat index levels are associated with higher risks of dehydration, impaired thermoregulation, and heat-related illness, as well as reduced cognitive and physical performance, particularly among children [42]. This distinction is especially relevant for children, who have lower sweat rates than adults and therefore depend more on efficient evaporation to shed heat, an outcome that high ambient humidity progressively suppresses [18]. Because the heat index rises with humidity, it captures this heightened vulnerability more directly than air temperature alone, and it has accordingly been used as the primary metric in prior evaluations of schoolyard shade and greening interventions [42,43]. However, despite their relevance for children's daily thermal exposure, schoolyards have rarely been the object of dedicated heat assessments.

2.4. Statistical analyses

To address the research questions on thermal exposure and thermal comfort in schoolyards, we applied a set of Generalized Additive Models (GAMs) with a Gaussian error distribution and identity link. GAMs were selected to flexibly capture non-linear diurnal temperature dynamics while accounting for differences in surface materials, shading conditions, and school-level heterogeneity. All analyses were conducted separately for air temperature and heat index in Python 3.10 [44].

Across all models, hour of day was included as a cyclic smooth term to represent diurnal thermal patterns. To reduce high-frequency temporal autocorrelation among the 2-min field readings, sensor data were first resampled to approximately 30 min resolution before model fitting. School was included as a fixed effect to control for site-specific characteristics such as local climate, urban context, and schoolyard configuration. Model-based comparisons were performed using estimated marginal means (EMMs), which represent model-adjusted average values for each category after accounting for other variables in the model, and marginal contrasts with 95% confidence intervals. Unless otherwise specified, contrasts were restricted to observed combinations of surface type, shading condition, and school in order to avoid extrapolation beyond the empirical data. Finally, we analyzed the residuals for each GAM to assess model assumptions.

2.5. Land surface effects on air temperature and heat index (Global GAM)

First, we fitted a global GAM to estimate the average effect of surface type on air temperature (or heat index) across all schools. The objective of this model was to identify surface materials associated with higher air temperature and heat index, while controlling for diurnal variation and school-level differences.

The global model is expressed as:

$$\mathrm{Temp}_i = \beta_0 + f_1(\mathrm{hour}_i) + f_2(\mathrm{lat\ lon}_i) + \mathrm{Surface}_i + \mathrm{Shade}_i + \mathrm{School}_i + \varepsilon_i$$

where $Temp_i$ (or $Heat\ Index_i$) represents the observed thermal measurement at observation i. $f_1\ (hour_i)$ is a smooth function of hour of day capturing non-linear diurnal patterns, $f_2\ (Lat\ Lon)$ is a bivariate smooth accounting for spatial structure representing the specific location of each sensor, Surface and Shade are categorical predictors. School is included as a fixed effect to control for site-specific differences, and $\varepsilon_i$is the error term. From this model, EMMs and pairwise contrasts were used to compare thermal conditions among surface types, marginalizing over observed shading conditions and hours of the day.

2.6. Shade-associated differences across surface materials

Second, to assess context-specific thermal responses, we fitted GAMs restricted to observed surface–shade combinations within schools. This approach avoids extrapolation to unobserved conditions and allows the effect of shade to be evaluated only where sun, partial shade, and shade observations were available for a given surface within a given school (See supplementary material to see specific combinations in each school).

These models follow the general structure:

$$\mathrm{Temp}_{i,s} = \beta_0 + f_1(\mathrm{hour}_i) + \mathrm{Surface}_i \times \mathrm{Shade}_i + \mathrm{School}_i + \varepsilon_i$$

where terms are defined as above. Model-based marginal contrasts were used to estimate the difference in air temperature and heat index between shaded and sun-exposed conditions (Shade − Sun) for each surface type within each school. Only surface–shade combinations with observations under three conditions were included in the contrasts, ensuring that estimated effects were based exclusively on empirical comparisons.

2.7. Comparison of natural versus artificial shade

School- and surface-specific generalized additive models (GAMs) were fitted to quantify differences in thermal conditions between natural and artificial shade while accounting for diurnal variability. For each school–surface combination, models included a cyclic smooth function of hour of day and a categorical effect for shade type.

$$\mathrm{Temp}_{i,s,k} = \beta_{0,s,k} + f_{cyc}(\mathrm{hour}_i) + (\mathrm{ShadeType}_i) + \varepsilon_i$$

Where $Temp_i$ (or $Heat\ Index_i$) represents air temperature or heat index measured at the observation i within the school s and the surface k. The term f_{cyc} denotes a cyclic smooth function of hour of day, capturing diurnal thermal patterns, and *ShadeType* is a categorical variable distinguishing natural from artificial shade.

Analyses were restricted to school–surface combinations where both shade types were observed during overlapping hours of the day, thereby avoiding temporal extrapolation. For each valid combination, model-based marginal contrasts were used to estimate differences in thermal conditions between natural and artificial shade (Natural − Artificial), with uncertainty quantified using bootstrap-derived 95% confidence intervals.

3. Results

3.1. Background regional diurnal temperature patterns during monitoring periods

Weather data (Weatherbit.io, [12]) revealed clear regional differences in the diurnal evolution of air temperature during the school monitoring periods (Fig. 3). Inland regions exhibited the highest temperatures and the latest daily temperature peaks. In the San Bernardino

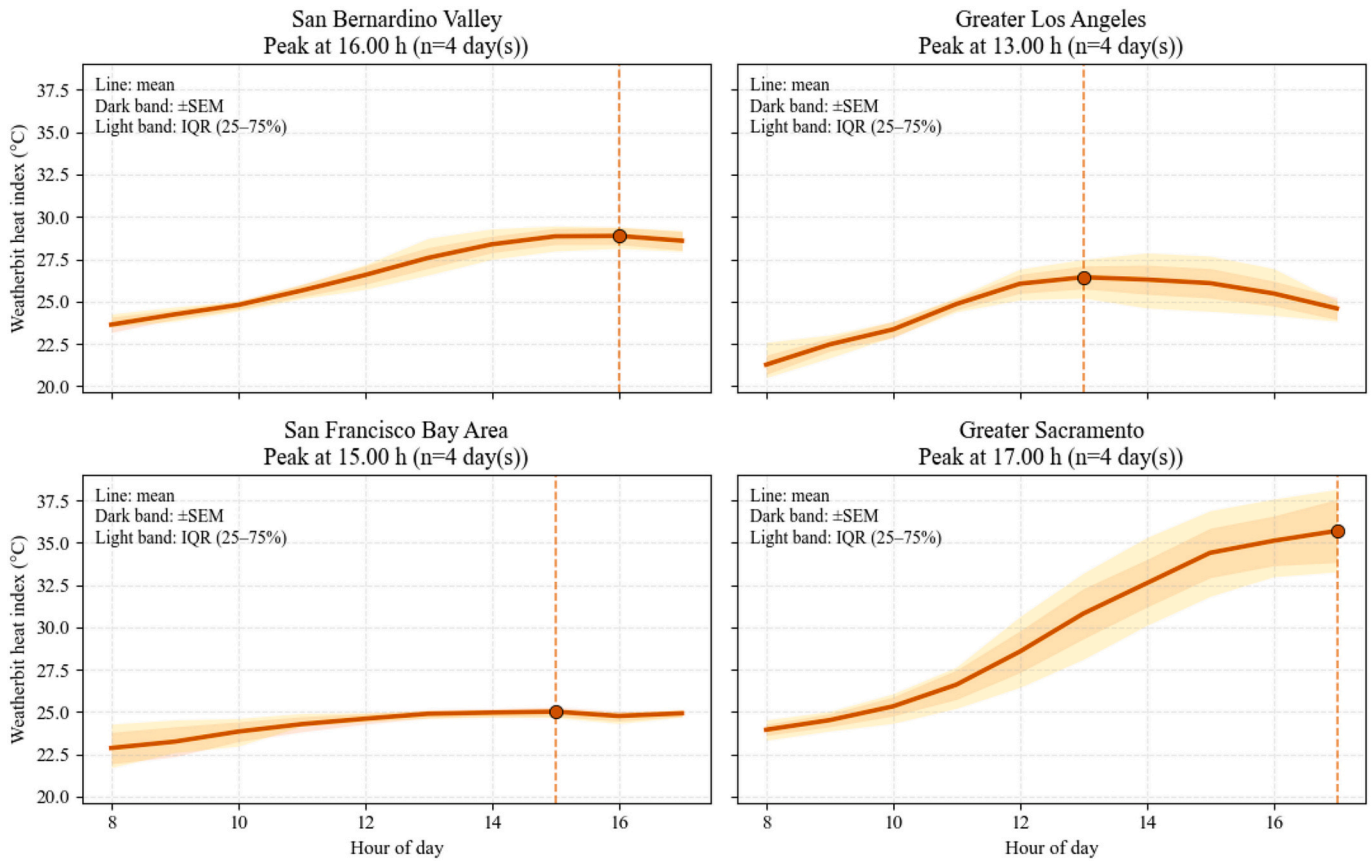


Fig. 3. Mean diurnal (8:00–17:00 h) heat index derived from Weatherbit data [12] across study areas in California. Red lines represent hourly means, and shaded bands indicate the interquartile range (25th–75th percentile). (For interpretation of the references to colour in this figure legend, the reader is referred to the web version of this article.)

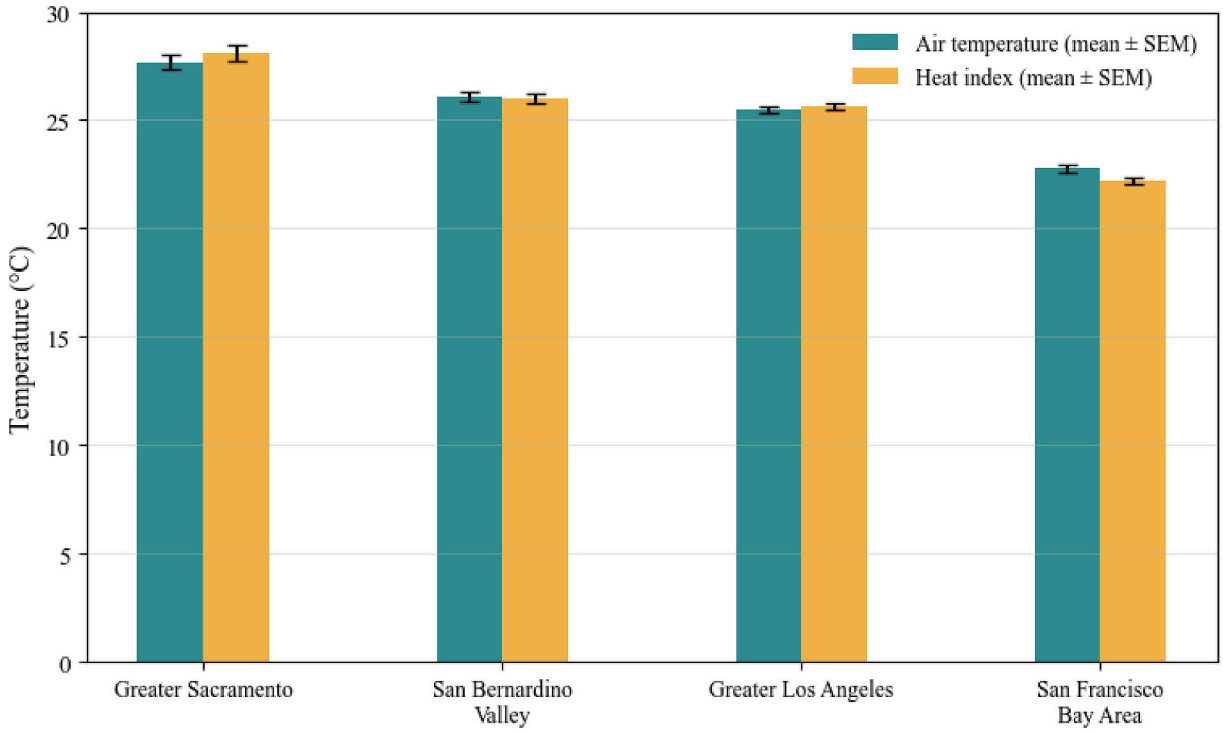


Fig. 4. Mean air temperature and heat index across climatic regions of California. Bars represent regional means, and error bars indicate ± SEM (Standard Error of the Mean).

Valley, air temperature increased steadily throughout the day, reaching a late-afternoon maximum at approximately 16:00 h (mean ≈ 30 °C ± standard error of measurement (SEM) 0.70 °C), with a heat index of 28.9 °C ± SEM 0.5 °C, indicating sustained warming across school hours. A similar pattern was observed in the Greater Sacramento area, where temperatures also peaked around 17:00 h (mean ≈ 30.9 °C ± SEM 1.86 °C), with a heat index of 35.7 °C ± SEM 1.86 °C. However, values tended to stabilize or slightly decline thereafter.

In contrast, schools in the Greater Los Angeles area exhibited an earlier temperature peak around 13:00 h (mean air temperature ≈ 25 °C ± SEM 0.84 °C) with a corresponding mean heat index of 26.4 °C ± SEM 0.67 °C, followed by a gradual stabilization or modest decrease during the afternoon hours. The San Francisco Bay Area showed the lowest overall temperatures and a more moderate diurnal cycle, with peak values occurring around 15:00 h (mean air temperature ≈ 22 °C ± SEM 1.01 °C) with a mean heat index of 22.2 °C ± SEM 0.28 °C, consistent with its coastal climatic influence.

When aggregated by region, field-based measurements of mean air temperature and heat index were highest in the Greater Sacramento area, followed by the San Bernardino Valley, while coastal regions exhibited milder conditions and lower average values (Greater Los Angeles and San Francisco Bay Area; Fig. 4). Extreme heat index values (>40 °C) were observed almost exclusively in inland regions (See supplementary material for descriptive statistics for each school).

Substantial variability was observed among schools. Mean air temperature across schools ranged from 21.4 °C ± SEM 2.87 °C (School 05) to 33.5 °C ± SEM 6.38 °C (School 08), while mean heat index ranged from 20.6 °C ± SEM 2.89 °C to 35.1 °C ± SE 7.56 °C across the same sites. Several schools experienced extreme thermal conditions, with maximum heat index values exceeding 40 °C at two schools (Schools 06 and 07), and a maximum recorded heat index of 48.6 °C at School 08. Wind speed, recorded by the Kestrel sensors, was generally low across all schools and sampling periods (mean = 1.17 ± 0.95 m/s; 95th percentile = 3.00 m/s), consistent with calm-to-light-breeze conditions, providing context for the limited potential for wind-driven air mixing between adjacent surface types during most of the monitoring period.

3.2. Differences in near-surface air temperature and heat index among surface types

The GAM explained a large proportion of the observed variability in both near-surface air temperature (pseudo-R^2 = 0.76) and heat index (pseudo-R^2 = 0.78). Spatial location and hour of day were the dominant contributors, reflecting strong regional climatic gradients and pronounced diurnal dynamics (see supplementary material: GAMs). After accounting for these spatial–temporal effects, surface material and shade condition remained statistically significant predictors in both models, indicating additional explanatory power beyond background climate and time-of-day effects. We examined residual autocorrelation and found lag-1 values of $r = 0.63$ for near-surface air temperature and $r = 0.61$ for heat index, declining to r ≈ 0.40 and 0.37 at lag-2. To ensure appropriate confidence intervals, we re-ran the bootstrap with sensor-day blocks rather than individual observations. The point estimates and intervals remained consistent, confirming the robustness of these findings. The relatively higher effective degrees of freedom (EDoF) associated with surface material (EDoF ≈ 5.6) suggest a complex and heterogeneous influence across surface types. In contrast, the lower EDoF for the shade condition (EDoF ≈ 1.5–1.0) indicates a more consistent, near-association with lower thermal exposure. Given that both models were fitted in parallel, it is worth noting that air temperature and heat index were highly correlated across all sensors (Pearson $r = 0.9$); however, relative humidity produced a measurable divergence within the 25–35 °C range typical of outdoor exposure, with heat index exceeding air temperature by up to 4–5 °C at the highest-humidity observations, and 9.6% of all two-minute observations falling into a different heat-stress category depending on which metric was used.

3.3. Temperature

Near-surface air temperature differed clearly among surface types (Fig. 5). Artificial turf exhibited the highest estimated marginal mean near-surface air temperature (EMM = 28.12 °C; 95% CI: 27.93–28.32 °C), followed by metal surfaces (EMM = 27.75 °C; 95% CI: 27.57–27.96 °C), although the latter were only present in a single school (School 03). Rubber surfaces and bare soil also showed relatively high near-surface air temperatures (EMM = 26.79 °C and 26.78 °C, respectively), closely followed by concrete (EMM = 26.63 °C).

Intermediate values were observed for mulch and asphalt, with similar estimated marginal means (EMM ≈ 26.18–26.20 °C). In contrast, vegetated and more permeable surfaces exhibited lower near-surface air temperatures. Grass showed reduced near-surface air temperatures (EMM = 25.93 °C; 95% CI: 25.74–26.13 °C), while plastic surfaces had the lowest estimated marginal means overall (EMM = 25.49 °C; 95% CI: 25.30–25.69 °C). To better capture site-specific variability, surface effects were also examined at the school level (Table 3 and Table 4).

Substantial heterogeneity in surface-specific thermal responses was observed among schools. For example, rubber-based surfaces exhibited some of the highest near-surface air temperatures, particularly in schools such as School 07, where rubber reached an estimated marginal mean (EMM) of 33.90 °C, closely followed by soil (33.89 °C) and concrete (33.74 °C), indicating consistently high thermal exposure across multiple surface types. In inland schools such as School 02 and School 08, soil emerged as the warmest near-surface air temperature, reaching EMMs of 28.89 °C and 28.16 °C, respectively, followed by concrete and mulch.

Notably, even in schools located in cooler coastal regions, certain materials exhibited elevated near-surface air temperatures. For instance, metal surfaces in School 03 reached an EMM of 25.79 °C, while artificial turf in School 05 reached 23.00 °C.

3.4. Heat index

Patterns observed for heat index were broadly consistent with those for air temperature, with EMM ranging from 25.59 to 28.05 °C across surface types (Fig. 6). These estimates represent model-based averages across all schools and may include extrapolation for surface types that were only present in a limited number of sites (e.g., artificial turf and metal). Artificial turf exhibited the highest heat index (EMM = 28.05 °C; 95% CI: 27.84–28.27 °C), followed by metal surfaces (EMM = 27.79 °C; 95% CI: 27.57–28.01 °C), although the latter were only present in a single school. Rubber and bare soil also showed elevated heat index values (EMM = 26.84 °C and 26.81 °C, respectively), followed by concrete (EMM = 26.67 °C). Intermediate values were observed for mulch and asphalt, while grass (EMM = 25.97 °C) and plastic surfaces (EMM = 25.59 °C) exhibited the lowest heat index levels.

Despite the relatively moderate average summer conditions during the measurement period, substantial variability in thermal exposure emerged across schools (Table 4). The highest estimated heat index values were observed in School 07, where multiple surfaces exhibited consistently elevated conditions, with rubber (EMM = 35.54 °C; 95% CI: 34.95–36.06 °C), soil (35.51 °C), and concrete (35.37 °C) all reaching levels within the extreme caution category. In inland schools such as School 08 and School 02, soil consistently emerged as the warmest surface, with EMMs of 28.49 °C and 28.20 °C, respectively, followed by concrete. Across several schools, conditions fell within the Caution range (27–32 °C), including School 04, where rubber reached 27.38 °C, and School 08 and School 02, where soil and mulch ranged between approximately 27.7 and 28.5 °C. In contrast, schools such as School 03, School 01, and School 06 exhibited lower estimated heat index values (EMM ≈ 24–26 °C), reflecting milder average conditions. Notably, even in cooler coastal settings, certain materials exhibited relatively elevated heat index values similar to the air temperature effect.

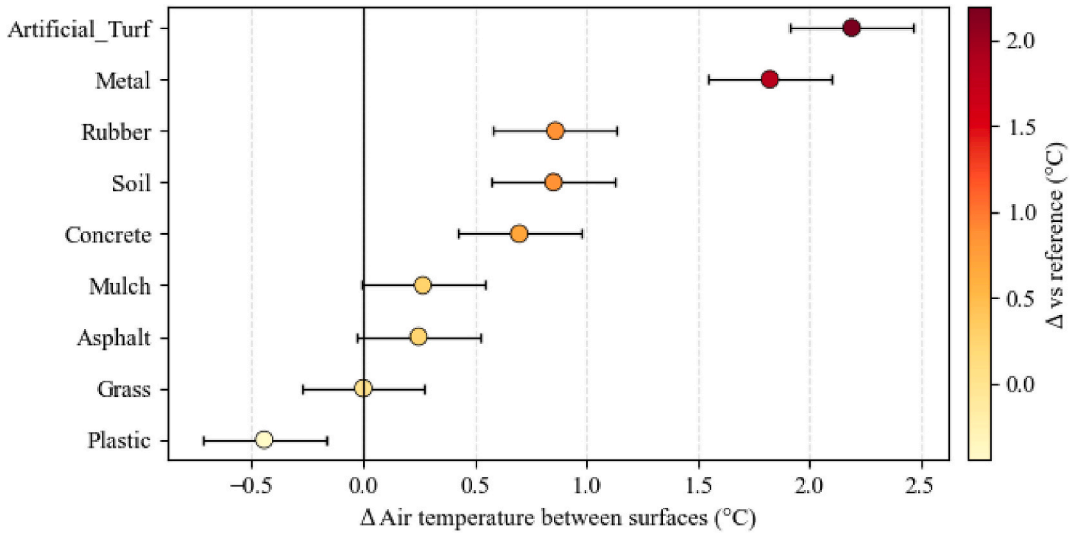


Fig. 5. Differences (Δ) in estimated marginal mean air temperature across surface types relative to the reference surface (Grass). Points represent model-derived contrasts from the GAM, and horizontal error bars indicate 95% confidence intervals. Grass temperature is used as a reference.

Table 3
Marginal effect of surface on the near-surface air temperature. EMM: Estimated marginal means. CI: 95% confidence intervals.

School number	Surface	EMM (°C)	CI95_low (°C)	CI95_High (°C)
01	Concrete	25.70	25.27	26.12
02	Soil	28.89	28.43	29.38
03	Metal	25.78	25.32	26.28
04	Rubber tiles	26.95	26.47	27.38
05	Artificial turf	22.99	22.52	23.40
06	Rubber tiles	26.18	25.76	26.51
07	Rubber tiles	**33.90**	**33.34**	**34.38**
08	Soil	28.16	27.79	28.52

Table 4
Marginal effect of surface on the heat index. EMM: Estimated marginal means. CI: 95% confidence intervals.

School number	Surface	EMM (°C)	CI95_low (°C)	CI95_High (°C)
01	Concrete	25.80	25.34	26.42
02	Soil	28.20	27.72	28.72
03	Metal	25.80	25.34	26.24
04	Rubber tiles	27.37	26.87	27.83
05	Artificial turf	22.19	21.70	22.62
06	Rubber tiles	25.85	25.40	26.21
07	Rubber tiles	**33.90**	**34.95**	**36.06**
08	Soil	28.48	28.09	28.86

3.5. Shade-associated differences in near-surface air temperature and heat index

A total of 50 surface-specific contrasts were evaluated across eight schools, including 13 Shade–Sun, 20 Partial Shade–Sun, and 17 Shade–Partial Shade comparisons (see Supplementary Materials). Across observations under sun and shade conditions, shaded locations consistently exhibited lower thermal exposure than sun-exposed areas. For the shade–sun contrast, shade-associated reductions in recorded near-surface temperature were observed in all eligible school–surface combinations (100% with 95% bootstrap intervals entirely below zero), encompassing seven schools (no shade–sun contrast reported in School 05). Shade-associated differences ranged from −2.37 to −0.08 °C for air temperature (median − 1.23 °C) and from −2.52 to −0.12 °C for heat index (median − 1.44 °C), indicating consistently lower recorded values under full shade.

Partial shade, often related with shade provided by buildings, showed a more heterogeneous response. For the partial shade–sun contrast, shade-associated reductions were detected in 16 out of 20 comparisons (80%) for air temperature and 17 out of 20 comparisons (85%) for heat index. Effect sizes were smaller and more variable, ranging from −1.96 to +1.43 °C for near-surface air temperature (median − 0.05 °C) and from −2.23 to +1.68 °C for heat index (median − 0.06 °C). In several cases (e.g., schools in Greater Sacramento), partial shade was associated with higher heat index values than full sun (up to +0.73 °C), particularly where sensors were located close to built structures, suggesting localized heat retention or reduced ventilation.

Direct comparisons between full and partial shade (shade–partial shade) further supported a graded shade response. Lower recorded values under full shade relative to partial shade were observed in 13 out of 17 comparisons (76%) for both near-surface air temperature and heat index. Maximum reductions reached up to −2.23 °C for near-surface air temperature and − 2.80 °C for heat index.

At the individual school level, complete shade was consistently associated with lower thermal exposure compared to sun-exposed conditions (Table 5).

The estimated shade-associated difference in recorded near-surface temperature (ΔShade–Sun) ranged from −0.23 °C to −2.37 °C for near-surface air temperature and from −0.30 °C to −2.44 °C for heat index. The largest reductions were observed at School 02 (−2.37 °C near-surface air temperature; −2.44 °C heat index) and School 04 (−2.16 °C heat index), whereas schools in the San Francisco Bay Area exhibited more modest shade-associated differences (< −0.35 °C).

3.6. Differences between natural and artificial shade

Across 12 matched surface–school comparisons (Fig. 7), differences between natural and artificial shade were generally small and highly variable for both near-surface air temperature and heat index. For near-surface air temperature, only two of twelve comparisons (16.7%) showed a statistically significant shade-associated difference under natural shade, with reductions of −1.95 °C on grass surfaces at School 08 and − 1.48 °C on concrete surfaces at School 06. In the remaining cases, confidence intervals overlapped zero, indicating no clear differences between shade types.

For the heat index, the effect was even more limited, with only one out of 12 comparisons (8.3%) showing a significant difference favoring natural shade, again observed on grass surfaces at School 08 (−2.37 °C).

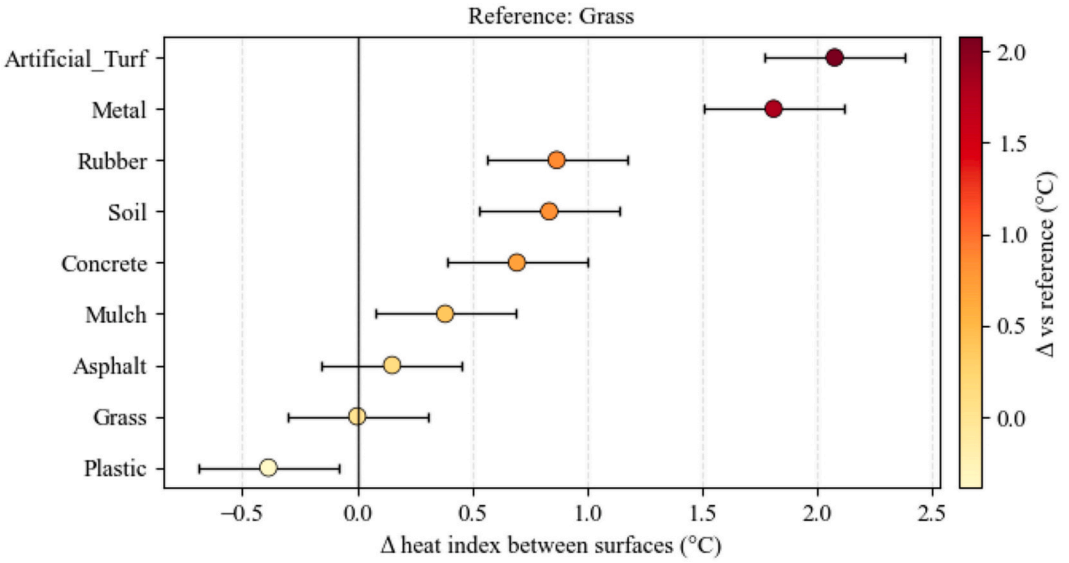


Fig. 6. Differences (Δ) in estimated marginal mean heat index across surface types relative to the reference surface (Grass). Points represent model-derived contrasts from the GAM, and horizontal error bars indicate 95% confidence intervals. Grass temperature is used as a reference.

Table 5
Delta in recorded near-surface temperature and heat index associated with shade.

School number	Mean ΔShade − Sun	
	Near-surface air Temperature (°C)	Heat index (°C)
02	−2.37	−2.44
04	−1.85	−2.16
01	−1.23	−1.44
07	−0.99	−1.25
08	−0.80	−1.11
03	−0.32	−0.32
06	−0.23	−0.30

Although additional comparisons showed negative mean differences, their confidence intervals overlapped zero.

4. Discussion

4.1. Near-surface thermal exposure, land cover, and surface materials

California schoolyards are frequently dominated by pavement, with limited vegetation, exposed surfaces, and little available shade [5,45]. This is especially important because cities already experience elevated temperatures due to the urban heat island effect [4]. This situation is particularly concerning for children's well-being, as their anatomical and physiological characteristics make them more vulnerable to reduced thermoregulation capacity [18]. Our study examined how surface type and shade conditions influence heat index and near-surface air temperature across eight schools in California. Overall, the strongest driver of these variables (air temperature and heat index) is the geographical location of each school. Inland schools tend to experience higher temperatures and lower relative humidity, whereas coastal schools are moderated by marine influences, particularly fog during summer (Table 1).

After controlling for region and location, we observed consistent influences of ground surface type and shade condition on school microclimates. Data was collected during relatively mild weather compared to recent extreme heat events in California (Table 1); therefore, the thermal conditions reported here are likely to represent conservative estimates of the thermal exposure children may experience on school campuses. Even under moderate conditions, several schools reached heat index values within the Caution (27–32 °C) and Extreme Caution categories (32–41 °C), with some observations exceeding (>40 °C). As heat waves become more frequent and intense [38,39,46], high heat index situations are likely to occur more often and with greater severity. For instance, School 07 in Greater Sacramento experienced substantially higher absolute temperatures (mean = 31.5 °C; maximum = 38.8 °C), resulting in high heat index values primarily driven by ambient heat. Nevertheless, several schools with lower maximum temperatures still reached heat index levels within the caution range (e.g., School 02, School 08 and School 06), indicating that heat stress can arise from different combinations of regional climate, humidity, and surface characteristics, rather than absolute temperature alone. These highest values were typically recorded during peak afternoon hours, representing short duration but potentially hazardous exposure events towards the end of the school day or during afterschool programs. Peak afternoon thermal exposure highlights the importance of providing adequate shade during late-day activities, when children often remain outdoors for extracurricular activities or afterschool programs. Our results underscore the importance of considering both background regional weather conditions and surface microclimatic effects when assessing thermal risk in schoolyards. However, interpretation of global marginal effects should be approached cautiously, as some surface types (artificial turf, metal and plastic) were present in only at one school in the main set. For instance, artificial turf was present in only three schools across the full dataset and in just one of the eight schools in the main sample, reflecting its relatively limited use in the studied campuses. Metallic surfaces were measured at only one location (School 03 in Greater Los Angeles), largely as a consequence of the randomized sensor placement design, although metal elements such as access ramps or platforms were present in several schools. Consequently, estimates for these materials may reflect extrapolated averages rather than broadly representative conditions across all sites.

Our findings highlight how strongly surface materials can shape local thermal exposure even when background temperatures are moderate. Despite some limited representation, the observed patterns are consistent with previous research documenting strong heat amplification over synthetic and metallic materials. At the single school where it was measured (School 05, San Francisco Bay Area), artificial turf showed the highest estimated heat index among the surfaces present (EMM = 28.12 °C), despite being located in a comparatively cool coastal climate; given this single-site representation, this finding should not be

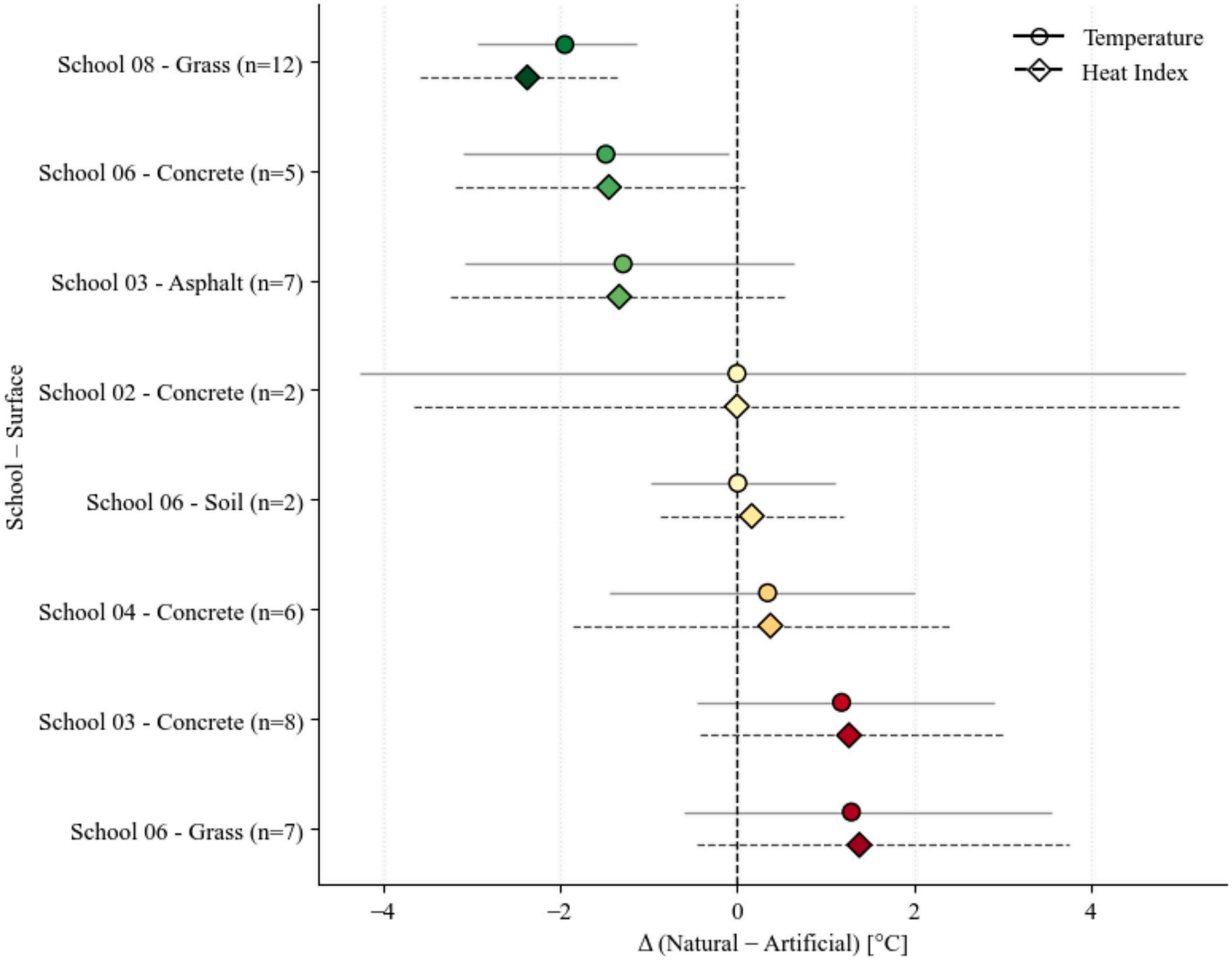


Fig. 7. Differences between natural and artificial shade in near-surface air temperature and heat index across school–surface combinations (n indicates the number of sensors contributing to each surface–shade). Points represent estimated differences (Δ = Natural − Artificial) derived from generalized additive models (GAMs), with horizontal lines indicating 95% bootstrap confidence intervals. Circles (solid lines) correspond to air temperature, and diamonds (dashed lines) to heat index.

generalized as a ranking applicable across schools. This highlights how surface material properties can influence local thermal environments alongside broader climatic conditions. Previous studies have similarly shown that artificial turf can be substantially hotter than natural grass, with midday surface temperatures (not near-surface air temperature) up to 182% higher and, in some cases, exceeding those of asphalt [47]. In addition to thermal concerns, artificial turf has been associated with the release of hazardous chemicals, posing potential exposure risks for children through inhalation and dermal contact [48,49]. These emissions may be further exacerbated under high-temperature conditions, as elevated surface temperatures can enhance the volatilization of organic compounds and increase exposure potential during periods of intense heat [49–51]. A similar pattern was observed for metallic surfaces, measured at a single sensor in a single school (School 03), it produced a comparatively high estimated heat index (EMM ≈ 28 °C) despite the school being among the coolest overall (mean air temperature = 22.1 °C); as with artificial turf, this result reflects a single site and should not be read as a general ranking across schools. This suggests that, under comparable environmental conditions, metallic materials can amplify heat stress more strongly than other ground covers, even in relatively cool climatic contexts [9] and present additional health hazards [15]. Consistent with these observations, the U.S. Consumer Product Safety Commission [52,53] recommends minimizing exposed metal playground elements or placing them under shade to reduce burn risk.

In the same vein, rubber tiles and rubber mats also showed elevated thermal exposure in our study, with some of the highest estimated marginal means (EMMs) across all surfaces. For instance, rubber tiles reached peak values in School 07 (EMM = 33.90 °C for near-surface air temperature; 35.54 °C for heat index), and remained among the warmest materials encountered in playground areas, often under full sun exposure or with limited artificial shade, where children spend a substantial portion of their outdoor time. Although these materials are widely recommended because of their energy-absorbing properties and injury-prevention benefits [53], they can retain heat more strongly than many traditional surfaces [54]. Under high temperatures, crumb rubber may emit toxic compounds and can deteriorate structurally under prolonged heat exposure. Previous playground studies have also shown that walking and standing on surfaces made of rubber can reach temperatures approaching burn thresholds under direct sunlight [9,55]. Consistent with these findings, recent thermal mapping identified rubber surfacing as one of the worst-performing playground materials, reaching surface temperatures up to 37 °C above air temperature and exceeding 80 °C under full sun exposure [56]. In contrast, plastic, also represented by two different locations within a single school, showed the lowest estimated heat index across all surfaces in the dataset, despite

being measured entirely under full sun exposure. This divergence from the pattern observed for artificial turf and metal, both recorded at comparably cool sites, is consistent with prior work showing that plastic-type playground materials (e.g., thermoplastic polyolefin) can be substantially cooler than rubber-crumb and synthetic turf surfacing under direct sun, likely reflecting differences in surface reflectivity and thermal absorption rather than shading [57].

Natural alternatives, including wood-based materials (e.g., mulch or engineered wood fiber), are often promoted as cooler substitutes [57]. Evidence suggests that these materials can exhibit lower surface temperature than ambient air, even under dry and sun-exposed conditions [57]. Contrary to that past research, our results indicate that mulch thermal performance is context-dependent. For instance, in Schools 01 and School 08 (both located inland), mulch exhibited lower heat index values compared to impervious surfaces (e.g., EMM = 25.49 °C and 28.04 °C, respectively), suggesting a potential cooling benefit. However, at School 02 (also inland located), mulch reached values comparable with bare soil or concrete. Bare soil, in particular, can act as a significant heat source, often reaching high near-surface temperatures under direct solar radiation due to its low albedo and limited evaporative cooling [58]. Sayão et al. [58] reported that bare soil surface temperature can exceed more than 40 °C of surface temperature under hot and dry conditions. Consistent with this, near-surface air temperature over soil was among the warmest surfaces in our dataset, particularly in Schools 02 and 08, and also appeared at intermediate levels across other sites. However, bare soil was not found in primary play areas; rather, it was found in degraded zones where grass seemed to have been present before. Only in School 05 were soil surfaces intentionally present, primarily along garden trails covered with dirt or sand.

4.2. Shade-associated differences in thermal exposure across California schoolyards

Our findings highlight that material choice alone is insufficient to determine thermal performance and that the presence and quality of shade play a critical role in modulating surface heat exposure. Guidance from the National Program for Playground Safety (NPPS) emphasizes both natural and artificial shade as practical strategies to reduce solar radiation, lower near-surface temperatures, and mitigate heat stress in children [59]. Similarly, Vanos et al. [9] reported substantial benefits of both shade types in reducing ultraviolet radiation (UVR) exposure during outdoor activities. Additional studies have shown that shaded playground surfaces can remain well below hazardous temperature thresholds [60,61].

Consistent with these studies, across all schools and surface types, shade in our schools was consistently associated with lower recorded thermal exposure, reinforcing its role as a key mitigation strategy. For near-surface air temperature, the shade-associated difference in recorded near-surface temperature relative to sun exposure ranged from −0.30 °C to −2.36 °C, with the largest reductions observed at School 02 (−2.36 °C) and School 04 (−2.20 °C). For heat index, shade-associated reductions were observed across a broader set of schools, with reductions exceeding 2 °C in two schools (Schools 02, and 04), and greater than 1 °C in five schools. These magnitudes are consistent with previous studies reporting relatively modest reductions in temperature under shade conditions. For example, Cheung & Jim [24] reported an average daytime air temperature cooling of ∼0.6 °C under tree shade and ∼ 0.2 °C under concrete shade in Hong Kong, a city characterized by hot, humid summers and mild, relatively dry winters. Additionally, Middel & Krayenhoff [62] found that different urban shade configurations (street trees and photovoltaic panels) typically reduced air temperature by less than 1.5 °C, even under extreme heat conditions in the semi-arid region of Tempe, Arizona.

Shade-associated reductions were observed across both vegetated and impervious surfaces. Over grass, shade was associated with lower near-surface air temperature and heat index, possibly reflecting the combined influence of reduced solar radiation and evapotranspiration, a mechanism widely documented in urban climate studies [28,60]. However, these effects were not limited to vegetated surfaces. Impervious materials such as concrete also exhibited substantial reductions under shade. Even under relatively moderate climatic conditions (coastal metropolitan regions), shaded areas showed measurably lower thermal exposure, with differences of at least ∼0.5 °C observed in some sites (e.g., School 03). At the same time, the variability observed across schools and regions indicates that the effectiveness of shade is strongly context-dependent, reflecting interactions between surface characteristics and broader climatic conditions.

4.3. Relative cooling performance of natural versus artificial shade

In our study sites, shade was provided by a combination of sources (see Supplementary Materials for some examples), including tree canopies (natural shade), as well as built elements such as building shadows, permanent shade structures (e.g., open-sided pavilions covering lunch areas), and temporary installations (e.g., shade tents over playgrounds). These shade types differ in their geometry, material properties, and interaction with solar radiation, which in turn affect both the intensity and temporal stability of shading.

We did not detect consistent differences between natural and artificial shade in their cooling performance. Although there was a general tendency for natural shade to be associated with slightly larger reductions, this pattern was not consistent across schools or surface types. In part, this reflects the limited number of comparable surface/shade combinations available in the dataset. For example, in some schools (e.g., School 01), shade was provided mostly by trees over grass, and equivalent artificial shade was not present there, limiting direct comparisons. Among the subset of schools where both shade types occurred over comparable surfaces, natural shade showed larger reductions than artificial shade in only a few cases (School 03 on Asphalt, School 06 on Concrete, and School 08 on Grass), and these differences were not consistently observed within the same surface category.

These findings align with previous studies reporting relatively small or non-significant differences between natural and artificial shade in terms of air temperature or thermal indices [23,24,27,63]. However, other studies suggest that natural shade may provide stronger cooling than artificial structures. For instance, Shashua-Bar et al. [28], in a California context, found that tree shade, particularly over grass, can be especially effective due to the combined effects of radiation interception and evapotranspiration, whereas artificial shading may reduce radiation but not always produce equivalent cooling. Similarly, Colter et al. [60] reported greater thermal benefits under vegetated shade compared to built structures.

4.4. Limitations and Ways Forward

Several limitations should be considered when interpreting our results. First, surface classification was based on visual inspection, which does not capture variability in material properties within each category. For example, the asphalt category may include surfaces with different albedo, permeability, or thermal properties. This within category heterogeneity likely introduces additional variability and suggests that more detailed material characterization would be valuable in future studies. Second, our measurements were conducted during the summer of 2025, which was relatively mild across California. Consequently, our results reflect moderate rather than extreme heat conditions. While this provides a useful baseline, it may underestimate the magnitude of thermal exposure in elementary-age children and the shade-associated differences under more intense heat events. Additionally, because coordinating field access across independent school districts made concurrent sampling infeasible, schools were monitored across a two-month period (July–August), during which solar declination shifted by approximately 9.7°; however, sampled maximum temperatures deviated

from 30-year historical norms by only −0.7 °C on average across schools, suggesting limited systematic effect on our results. Third, the comparison between natural and artificial shade was constrained by the limited number of sites where both shade types occurred over the same surface materials. Identifying paired conditions in schoolyards is challenging due to their inherent spatial heterogeneity. Fourth, shade was classified categorically (shade, partial shade, sun; natural vs. artificial) based on field observation, but shade quality, such as canopy density, transmissivity, or sky view factor, was not measured as a continuous variable. Future work incorporating hemispherical photography or LiDAR-derived canopy metrics, ideally on a larger number of tree species with varying hydraulic and morphological traits, could help quantify how shade density modulates cooling magnitude beyond the categorical distinctions used here. Fifth, although wind speed was generally low across schools, we did not explicitly quantify or control for potential thermal bleeding or advection effects from adjacent, thermally dominant surfaces (e.g., small rubber mats surrounded by unshaded asphalt); footprint modeling or higher-resolution spatial sampling would be needed to fully characterize these micro-scale mixing effects. Sixth, our models included school as a fixed effect but did not specify a random effect for individual sensors, despite each sensor contributing repeated, temporally autocorrelated observations over the sampling period. A sensor-level block bootstrap conducted for the surface-school combinations with the widest original confidence intervals produced narrower, not wider, estimates, indicating that this simplification did not meaningfully understate uncertainty in these cases; we nonetheless recommend a formal mixed-effects framework with sensor as a random effect in future work. Seventh, air-temperature sensors were not radiation-shielded, reflecting the instrument's integrated design for simultaneous WBGT measurement, which requires the black-globe and natural-wet-bulb sensors to remain exposed, we therefore cannot rule out the presence of radiative bias in full-sun air-temperature and heat-index readings. Overall, advancing this line of research will require more detailed measurements capable of capturing multiple heat fluxes and radiation components, alongside more controlled comparisons of surfaces and shade characteristics.

Despite these limitations, this study provides valuable empirical evidence on how surface materials and shade conditions influence the thermal exposure in schoolyards. The results presented here can support decision-makers in prioritizing material selection and, importantly, in recognizing the role of shade as a heat mitigation strategy. While natural shade did not consistently outperform artificial shade in terms of the magnitude of recorded shade-associated differences in this study, trees remain essential components of urban landscapes due to the wide range of ecosystem services they provide in addition to shade. In school environments, trees support children's cognitive, physical, and social development [64–66]. Therefore, both surface material choice and integrations of diverse and effective shade strategies and co-benefits should be considered jointly in the design and management of climate-resilient schools in California.

CRediT authorship contribution statement

Luisa Velasquez-Camacho: Writing – review & editing, Writing – original draft, Visualization, Validation, Supervision, Software, Project administration, Methodology, Investigation, Formal analysis, Data curation, Conceptualization. **Natalie S. van Doorn:** Writing – review & editing, Supervision, Resources, Project administration, Methodology, Investigation, Funding acquisition, Conceptualization. **Lara A. Roman:** Writing – review & editing, Supervision, Resources, Project administration, Methodology, Funding acquisition, Conceptualization. **Iryna Dronova:** Writing – review & editing, Writing – original draft, Supervision, Project administration, Funding acquisition, Formal analysis. **Kirsten Schwarz:** Writing – review & editing, Supervision, Project administration, Funding acquisition, Formal analysis. **Jared Sisneroz:** Supervision, Investigation, Data curation. **Elizabeth Riedman:** Project administration, Investigation. **Levon M. Bigelow:** Project administration, Investigation. **Alessandro Ossola:** Writing – review & editing, Supervision, Project administration, Methodology, Investigation, Funding acquisition, Formal analysis, Data curation, Conceptualization.

Declaration of competing interest

The authors declare that they have no known competing financial interests or personal relationships that could have appeared to influence the work reported in this paper.

Acknowledgements

We thank the California Department of Forestry and Fire Protection and Green Schoolyards America, as well as the school tree study advisory committee, for their support and guidance throughout this project. We also acknowledge the work of numerous students from UC Davis, UC Berkeley, and UCLA with tree data collection. We are grateful to the school district staff who partnered on this research and allowed us to study their schools, including M Allegretti at Oakland Unified School District and Jay Kim at Colton Joint Unified School District. This study was made possible with funding from the USDA Forest Service Region 5 State, Private, and Tribal Forestry, as well as the USDA Forest Service Pacific Southwest Research Station (Agreement No. 23-CS-11272123-031 to UC Davis, 23-CS-11272123-029 to UCLA, and 23-CS-11272123-038 to UC Berkeley). Further funding was provided by the UCLA Luskin School of Public Affairs and the UC Davis College of Agricultural and Environmental Sciences. This study was supported in part by LMB's appointment to the United States Department of Agriculture (USDA) Forest Service (FS) Research Participation Program administered by the Oak Ridge Institute for Science and Education (ORISE) through an interagency agreement between the US Department of Energy (DOE) and the USDA (Interagency Agreement No. 23-IA-11272123-030). ORISE is managed by Oak Ridge Associated Universities (ORAU) under DOE contract number DE-SC0014664. AO is supported by Hatch Project No. CA-DPLS-2735-H.The opinions and findings expressed in this paper do not necessarily reflect the views of the funders and should not be construed to represent any official USDA or US Government determination or policy.

Appendix A. Supplementary data

Supplementary data to this article can be found online at https://doi.org/10.1016/j.cacint.2026.100507.

Data availability

Data will be made available on request.

References

[1] Antoniadis D, Katsoulas N, Tsirogiannis I, Kittas C. Effects of planting and structural configurations on human thermal comfort in a schoolyard. In: VI International Conference on Landscape and Urban Horticulture 1189; 2016. p. 229–34.
[2] Murphy CM, Howie EK, Barenie MJ, Weber KA, Thomsen MR. Examining relationships between U.S. children's physical activity levels during recess, school days, and weekend days. Prev Med Rep 2025;55:103120. https://doi.org/10.1016/j.pmedr.2025.103120.
[3] Ridgers ND, Saint-Maurice PF, Welk GJ, Siahpush M, Huberty J. Differences in physical activity during school recess. Journal of School Health 2011;81(9):545–51.
[4] Antoniadis D, Katsoulas N, Papanastasiou DK. Thermal environment of urban schoolyards: current and future design with respect to children's thermal comfort. Atmosphere 2020;11(11):1144. https://doi.org/10.3390/atmos11111144.
[5] Ng M, Coffelt J. Depaving California schools for a greener future. 2024.
[6] Pearson AL, Pfeiffer KA, Shortridge A, Clevenger KA. Schoolyard level inventory for describing the environment: linking high-resolution spatiotemporal data to the physical environment to understand children's physical activity behaviors. Journal of School Health 2025;95(6):410–22. https://doi.org/10.1111/josh.70008.

[7] Schulman A, Peters CA. GIS analysis of urban schoolyard landcover in three U.S. cities. Urban Ecosyst 2008;11(1):65–80. https://doi.org/10.1007/s11252-007-0037-4.

[8] Blanc N, Clauzel C, About C, Riché A-L, Gippet M, Bortolamiol S. Schoolyards greening for connecting people and nature: an example of nature-based solutions? Npj Urban Sustain 2025;5(1):64. https://doi.org/10.1038/s42949-025-00252-6.

[9] Vanos JK, Middel A, McKercher GR, Kuras ER, Ruddell BL. Hot playgrounds and children's health: a multiscale analysis of surface temperatures in Arizona, USA. Landscape and Urban Planning 2016;146:29–42. https://doi.org/10.1016/j.landurbplan.2015.10.007.

[10] Wu R, Fang X, Brown R, Liu S, Zhao H. Establishing a link between complex courtyard spaces and thermal comfort: a major advancement in evidence-based design. Build Environ 2023;245:110852.

[11] Moogk-Soulis C. Schoolyard heat Islands: a case study in Waterloo, Ontario. 2002.

[12] Weatherbit.io. Weatherbit weather data API. https://www.weatherbit.io; 2025.

[13] Chatzidimitriou A, Yannas S. Microclimate Development in Open Urban Spaces: The Influence of Form and Materials. Energy Build 2015;108:156–74. https://doi.org/10.1016/j.enbuild.2015.08.048.

[14] Lanza K, Alcazar M, Durand CP, Salvo D, Villa U, Kohl HW. Heat-resilient schoolyards: relations between temperature, shade, and physical activity of children during recess. Journal of Physical Activity and Health 2023;20(2):134–41. https://doi.org/10.1123/jpah.2022-0405.

[15] Choi Y, Chopra T, Smith D, Moulton S. Sun heated surfaces are an environmental hazard for young children. Perspect Public Health 2019;139(5):264–70. https://doi.org/10.1177/1757913919826600.

[16] Kennedy E, Olsen H, Vanos J, Vecellio DJ, Desat M, Richters K, et al. Reimagining spaces where children play: developing guidance for thermally comfortable playgrounds in Canada. Can J Public Health 2021;112(4):706–13. https://doi.org/10.17269/s41997-021-00522-7.

[17] Cordeiro AMR, Fialho J, Coelho C, Lameiras JM. Greening schools for climate resilience and sustainable co-design: a case study of thermal comfort in Coimbra, Portugal. Land 2025;14(10):1985. https://doi.org/10.3390/land14101985.

[18] Forsyth N, Solan T. It's getting hot in here: heat stroke in children and young people for paediatric clinicians. Paediatr Child Health 2022;32(12):471–5.

[19] Bloch S. Shade. Places Journal 2019. https://doi.org/10.22269/190423.

[20] Turner VK, Middel A, Vanos JK. Shade is an essential solution for hotter cities. Nature 2023;619(7971):694–7. https://doi.org/10.1038/d41586-023-02311-3.

[21] Georgi NJ, Zafiriadis K. The impact of park trees on microclimate in urban areas. Urban Ecosyst 2006;9(3):195–209.

[22] Gkaidatzi L-D, Tseliou A, Katsavounidou G, Zervas E. Investigation of the thermal environment in schoolyards under Mediterranean conditions. Contribution to bioclimatic conditions improvement with the application of mild interventions – the case study of a school within the urban environment. IOP Conf Ser Earth Environ Sci 2022;1123(1):012031. https://doi.org/10.1088/1755-1315/1123/1/012031.

[23] Middel A, AlKhaled S, Schneider FA, Hagen B, Coseo P. 50 grades of shade. Bull Am Meteorol Soc 2021;102(9):E1805–20.

[24] Cheung PK, Jim CY. Comparing the cooling effects of a tree and a concrete shelter using PET and UTCI. Build Environ 2018;130:49–61. https://doi.org/10.1016/j.buildenv.2017.12.013.

[25] Zare S, Hasheminejad N, Shirvan HE, Hemmatjo R, Sarebanzadeh K, Ahmadi S. Comparing Universal Thermal Climate Index (UTCI) with selected thermal indices/environmental parameters during 12 months of the year. Weather Clim Extremes 2018;19:49–57.

[26] Middel A, Selover N, Hagen B, Chhetri N. Impact of shade on outdoor thermal comfort—a seasonal field study in Tempe, Arizona International Journal of Biometeorology 2016;60(12):1849–61. https://doi.org/10.1007/s00484-016-1172-5.

[27] Ouyang W, Ren G, Tan Z, Li Y, Ren C. Natural shading vs. artificial shading: a comparative analysis of their cooling efficacy in extreme hot weather. Urban Clim 2024;55:101870. https://doi.org/10.1016/j.uclim.2024.101870.

[28] Shashua-Bar L, Pearlmutter D, Erell E. The cooling efficiency of urban landscape strategies in a hot dry climate. Landscape and Urban Planning 2009;92(3–4):179–86. https://doi.org/10.1016/j.landurbplan.2009.04.005.

[29] Ong F. The form of reform: School facility design implications for California educational reform. California Dept. of Education; 1997.

[30] Serrano-Jiménez A, Hiruelo-Pérez J, Ramírez-Juidias E, Barrios-Padura Á. Identifying design shortcomings and heat-island effects in schools located in warm climates: an outdoor environmental assessment procedure based on remote sensing tools. J Build Eng 2021;43:103209. https://doi.org/10.1016/j.jobe.2021.103209.

[31] Kesseli JE. The climates of California according to the Koppen classification. Geogr Rev 1942;32(3):476. https://doi.org/10.2307/210390.

[32] Oliphant AJ, Baguskas SA, Fernandez DM. Impacts of low cloud and fog on surface radiation fluxes for ecosystems in coastal California. Theor Appl Climatol 2021;144(1–2):239–52. https://doi.org/10.1007/s00704-021-03518-y.

[33] Woodside G, Ojo A, Palenscar K, Feldman E. Climate adaptation and resilience plan for San Bernardino Valley, California, USA. . EGU General Assembly 2025. doi:. 2025. https://doi.org/10.5194/egusphere-egu25-14474.

[34] Constantz BM, Stella JC, Holl KD. Diverging restoration pathways for overstory and understory communities in a Mediterranean-climate riparian ecosystem. Ecol Appl 2025;35(3):e70043. https://doi.org/10.1002/eap.70043.

[35] Zhang JJ, Byrd CE. Successful after-school programs: the 21st century community learning centers. Journal of Physical Education, Recreation & Dance 2006;77(8):3–12. https://doi.org/10.1080/07303084.2006.10597912.

[36] Afterschool Alliance. The latest research on the impact of afterschool and summer programs. 2024.

[37] Albaloul O, Kulinna PH, Schulke M, Min H, Kim J, Hassan U, et al. Comprehensive strategies for managing school-based physical activity during extreme heat. Journal of Physical Education, Recreation & Dance 2025;96(6):7–14. https://doi.org/10.1080/07303084.2025.2507573.

[38] Gershunov A, Guirguis K. California heat waves in the present and future. Geophys Res Lett 2012;39(18):2012GL052979. https://doi.org/10.1029/2012GL052979.

[39] Wang J, Guan Y, Wu L, Guan X, Cai W, Huang J, et al. Changing lengths of the four seasons by global warming. Geophys Res Lett 2021;48(6):e2020GL091753. https://doi.org/10.1029/2020GL091753.

[40] International Organization for Standardization. Ergonomics of the thermal environment: assessment of heat stress using the WBGT (Wet Bulb Globe Temperature) index (ISO 7243:2017). International Organization for Standardization; 2017.

[41] Anderson GB, Bell ML, Peng RD. Methods to calculate the heat index as an exposure metric in environmental Health Research. Environ Health Perspect 2013;121(10):1111–9. https://doi.org/10.1289/ehp.1206273.

[42] Lanza, K., Alcazar, M., Hoelscher, D. M., & Kohl, I. H. W. (2020). Effects of trees, gardens, and trails on heat index and child health: design and methods of the green schoolyards project. In Review doi:10.21203/rs.3.rs-48960/v1.

[43] Shortridge A, Walker VI W, White DD, Guardaro MM, Hondula DM, Vanos JK. HeatReady schools: a novel approach to enhance adaptive capacity to heat through school community experiences, risks, and perceptions. Clim Risk Manag 2022;36:100437. https://doi.org/10.1016/j.crm.2022.100437.

[44] Python Software Foundation. Python 3.10 Programming Language. https://www.python.org; 2021.

[45] Velasquez-Camacho L, Willaredt M, Singh P, Ossola A. Bleeding green: California's schools are rapidly losing tree canopy cover. Urban Forestry & Urban Greening 2025;113:129117. https://doi.org/10.1016/j.ufug.2025.129117.

[46] Whittier L. Extreme Heat Takes a Toll on Californians' Health. Public Policy Institute of California (PPIC); 2024. , May 20, https://www.ppic.org/blog/extreme-heat-takes-a-toll-on-californians-health/.

[47] Cumberbatch IS, Richardson L, Grant-Bier E, Kayali M, Mbithi M, Riviere RF, et al. Artificial turf versus natural grass: a case study of environmental effects, health risks, safety, and cost. Sustainability 2025;17(14):6292. https://doi.org/10.3390/su17146292.

[48] Denk D, Frumkin H, Tandon P, Cohen H, Patterson E. The use of artificial turf in parks and schoolyards (Trust for Public Land Green Paper Series). Trust for Public Land; 2024. https://www.tpl.org.

[49] Kim H-H, Lim Y-W, Kim S-D, Yeo I-Y, Shin D-C, Yang J-Y. Health risk assessment for artificial turf playgrounds in school athletic facilities: multi-route exposure estimation for use patterns. Asian Journal of Atmospheric Environment 2012;6(3):206–21. https://doi.org/10.5572/ajae.2012.6.3.206.

[50] Cheng H, Hu Y, Reinhard M. Environmental and health impacts of artificial turf: a review. Environ Sci Technol 2014;48(4):2114–29. https://doi.org/10.1021/es4044193.

[51] Cheung PK, Livesley SJ. The microclimate, surface energy flux and human skin burn risks of artificial turf as compared to natural turf. Build Environ 2025;273:112679. https://doi.org/10.1016/j.buildenv.2025.112679.

[52] U.S. Consumer Product Safety Commission. Public playground safety handbook (Publication No. 325). U.S. Consumer Product Safety Commission; 2015. https://www.cpsc.gov/s3fs-public/325.pdf.

[53] U.S. Consumer Product Safety Commission. Public Playground Safety Handbook (Publication No. 325). U.S. Consumer Product Safety Commission; 2025. https://www.cpsc.gov/s3fs-public/325.pdf.

[54] Janajreh I, Hussain M, Elagroudy S, Moustakas K. Recycled tire granular for playground in hot regions: technical assessment. Journal of Material Cycles and Waste Management 2021;23(1):107–20. https://doi.org/10.1007/s10163-020-01100-8.

[55] Asquith C, Kimble R, Stockton K. Too hot to trot (barefoot)… a study of burns in children caused by sun heated surfaces in Queensland, Australia. Burns 2015;41(1):177–80. https://doi.org/10.1016/j.burns.2014.06.011.

[56] Katsavounidou G. The need for heat-resilient, natural play spaces: thermal mapping of playgrounds in a compact Mediterranean city. E3S Web Conf 2025;669:02006. https://doi.org/10.1051/e3sconf/202566902006.

[57] Pfautsch S, Wujeska-Klause A, Walters J. Outdoor playgrounds and climate change: importance of surface materials and shade to extend play time and prevent burn injuries. Build Environ 2022;223:109500. https://doi.org/10.1016/j.buildenv.2022.109500.

[58] Sayão VM, Dos Santos NV, De Sousa Mendes W, Marques KPP, Safanelli JL, Poppiel RR, et al. Land use/land cover changes and bare soil surface temperature monitoring in Southeast Brazil. Geoderma Reg 2020;22:e00313. https://doi.org/10.1016/j.geodrs.2020.e00313.

[59] CSA Group. Children's playground equipment and surfacing (Standard CAN/CSA-Z614:2020). CSA Group; 2020.

[60] Colter KR, Middel AC, Martin CA. Effects of natural and artificial shade on human thermal comfort in residential neighborhood parks of Phoenix, Arizona, USA. Urban Forestry & Urban Greening 2019;44:126429. https://doi.org/10.1016/j.ufug.2019.126429.

[61] Olsen H, Kennedy E, Vanos J. Shade provision in public playgrounds for thermal safety and sun protection: a case study across 100 play spaces in the United States. Landscape and Urban Planning 2019;189:200–11. https://doi.org/10.1016/j.landurbplan.2019.04.003.

[62] Middel A, Krayenhoff ES. Micrometeorological determinants of pedestrian thermal exposure during record-breaking heat in Tempe, Arizona: introducing the MaRTy observational platform. Sci Total Environ 2019;687:137–51. https://doi.org/10.1016/j.scitotenv.2019.06.085.

[63] Pfautsch S, Rouillard S, Wujeska-Klause A, Bae A, Vu L, Manea A, et al. School microclimates (p. 56) [Technical Report]. Western Sydney University; 2020.
[64] Li D, Sullivan WC. Impact of views to school landscapes on recovery from stress and mental fatigue. Landscape and Urban Planning 2016;148:149–58. https://doi.org/10.1016/j.landurbplan.2015.12.015.
[65] Matsuoka RH. Student performance and high school landscapes: examining the links. Landscape and Urban Planning 2010;97(4):273–82. https://doi.org/10.1016/j.landurbplan.2010.06.011.
[66] Raney MA, Daniel E, Jack N. Impact of urban schoolyard play zone diversity and nature-based design features on unstructured recess play behaviors. Landscape and Urban Planning 2023;230:104632. https://doi.org/10.1016/j.landurbplan.2022.104632.